AD-A179 976 TOMOGRAPHIC RECONSTRUCTION OF THREE-DIMENSIONAL FLOW OVER AIRFOILS. (U) SPECTRON DEVELOPMENT LABS INC COSTA MESA CA D MODARRESS ET AL. 10 MAR 87 SDL-87-2204-13F 1/1

UNCLASSIFIED ARO-19471.4-EG DAAG29-83-C-0012 F/G 20/4 NL

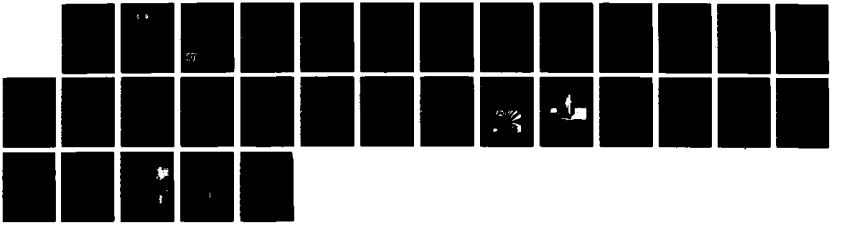

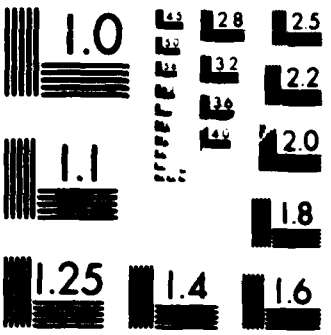

(2)

SEC

AD-A179 976

DTIC FILE COPY

REPORT DOCUMENTATION PAGE

DTIC ELECTE MAY 04 1987 S D

1a. REPORT SECURITY CLASSIFICATION: Unclassified	1b. RESTRICTIVE MARKINGS
2a. SECURITY CLASSIFICATION AUTHORITY	3. DISTRIBUTION/AVAILABILITY OF REPORT: Approved for public release; distribution unlimited.
2b. DECLASSIFICATION/DOWNGRADING SCHEDULE	
4. PERFORMING ORGANIZATION REPORT NUMBER(S): SDL No. 87-2284-13F	5. MONITORING ORGANIZATION REPORT NUMBER(S): ARO 19471.4-EG
6a. NAME OF PERFORMING ORGANIZATION: SPECTRON DEVELOPMENT LABS; 6b. OFFICE SYMBOL (If applicable)	7a. NAME OF MONITORING ORGANIZATION: U. S. Army Research Office
6c. ADDRESS (City, State, and ZIP Code): 3535 Hyland Avenue, Suite 102, Costa Mesa, CA 92626-1439	7b. ADDRESS (City, State, and ZIP Code): P. O. Box 12211, Research Triangle Park, NC 27709-2211
8a. NAME OF FUNDING/SPONSORING ORGANIZATION: U. S. Army Research Office; 8b. OFFICE SYMBOL (If applicable)	9. PROCUREMENT INSTRUMENT IDENTIFICATION NUMBER: DAAG29-83-C-0012
8c. ADDRESS (City, State, and ZIP Code): P. O. Box 12211, Research Triangle Park, NC 27709-2211	10 SOURCE OF FUNDING NUMBERS: PROGRAM ELEMENT NO; PROJECT NO; TASK NO; WORK UNIT ACCESSION NO

11 TITLE (Include Security Classification)
TOMOGRAPHIC RECONSTRUCTION OF THREE-DIMENSIONAL FLOW OVER AIRFOILS (UNCLASSIFIED)

12 PERSONAL AUTHOR(S)
Dariush Modarress, Hung Tan, and James D. Trolinger

13a. TYPE OF REPORT	13b TIME COVERED	14 DATE OF REPORT (Year, Month, Day)	15 PAGE COUNT
Final	FROM 3/15/83 TO 11/14/86	18 March 1987	30

16 SUPPLEMENTARY NOTATION
The view, opinions and/or findings contained in this report are those of the author(s) and should not be construed as an official Department of the Army position, policy, or decision, unless so designated by other documentation.

17 COSATI CODES		
FIELD	GROUP	SUB-GROUP

18. SUBJECT TERMS (Continue on reverse if necessary and identify by block number)
Tomography, Holography, Transonic, Fringe Digitization, Three-Dimensional

19 ABSTRACT (Continue on reverse if necessary and identify by block number)

Application of holographic tomography to the flow around the tip of a revolving airfoil is investigated. Data in the form of interferograms obtained at forty different angles obtained by AVRADCOM at NASA Ames were used to reconstruct the three-dimensional density field. An automated fringe analysis capability was developed to digitize, filter and repair the fringe patterns. The binary images of the interferograms were used as the input data to the reconstruction code. A new ART code based on the iterative refinement method of least squares solution was developed for tomographic reconstruction. Solutions were obtained for the density and velocity field at various heights above the blade. An important feature of the technique was found to be that with limited resolution (say 20 x 20), it was possible to repeatedly use the same code and zoom into regions surrounding important features of the flow and, hence, reconstruct the flow field in greater detail. This feature was used and the position of the shock wave over the wing was determined.

20 DISTRIBUTION/AVAILABILITY OF ABSTRACT: ☒ UNCLASSIFIED/UNLIMITED ☐ SAME AS RPT ☐ DTIC USERS	21 ABSTRACT SECURITY CLASSIFICATION: Unclassified
22a NAME OF RESPONSIBLE INDIVIDUAL	22b TELEPHONE (Include Area Code) / 22c OFFICE SYMBOL

DD FORM 1473, 84 MAR — 83 APR edition may be used until exhausted. All other editions are obsolete.

SECURITY CLASSIFICATION OF THIS PAGE
UNCLASSIFIED

TOMOGRAPHIC RECONSTRUCTION OF THREE-DIMENSIONAL FLOW OVER AIRFOILS

FINAL REPORT

Prepared by:

D. Modarress, H. Tan, and J. D. Trolinger
SPECTRON Development Laboratories, Inc.
3535 Hyland Avenue, Suite 102
Costa Mesa, California 92626-1439

SDL No. 87-2284-13F

18 March 1987

Prepared for:

U.S. Army Research Offices

Contract No. DAAG29-83-C-0012

SPECTRON
DEVELOPMENT
LABORATORIES, INC.

TABLE OF CONTENTS

LIST OF FIGURES

LIST OF TABLES

1.0 STATEMENT OF THE PROBLEM STUDIED

Application of holographic tomography to the flow around the tip of a revolving airfoil was investigated. Data in the form of interferograms obtained at different angles obtained by AVRADCOM at NASA Ames were used to reconstruct the three-dimensional density field. The data were obtained for the flow around a rotating NACA0012 airfoil at a tip mach number of 0.9 (See Figure 1). Each interferogram represented the integrated map of the optical path along a given orientation relative to the wing. A total of forty interferograms were used. A typical interferogram is shown in Figure 2. The final objective of the work was to reconstruct the density field around the tip of the rotating blade.

The work consisted of three stages:

a) Digitization of the interferograms in the phase maps.

b) Reconstruction of the set of integrated phase maps into a three-dimensional map of index of refraction.

c) Development of the density or mach number maps.

Each stage of the work is briefly described here:

a) Interferogram Digitization:

In the course of this project, a semi-manual and an automated technique for digitization of interferograms were developed. The hardware for the manual digitization consisted of a Tektronix 4112 display terminal and a graphic tablet connected to a VAX11/780. An efficient, menu-driven program for digitization of the interferograms was constructed. This technique was initially used for the digitization of the interferograms.

An automated image analyzing system was later developed. The hardware consisted of an IBM/AT personal computer, a video camera and a frame grabber. It had a 512 x 512 pixel resolution which could digitize at 30 frames per second rate. The fringe digitization hardware is shown in Figure 2.

The software consisted of three major sets of programs. The first set of the processing software included most of the standard "textbook" image processing procedures[1] such as image averaging, filtering, enhancement, zooming, mirror imaging for the axisymmetric problem along with Sobel or Robert edge operators. This set of programs was supported by a commercially available image processing software product.

The second program set was developed to determine fringe center-line coordinates according to the local gray scale distribution. This program was able to detect fringes with relatively poor visibility and with variable background gray scale.

The last program was the fringe detection algorithm which transformed the individual fringe line information into a phase map for the entire pixels. This was achieved by surface spline interpolation technique[2], an efficient technique to interpolate between sparse or nonuniformly spaced data points. It solves the equation for elastic deformation of a plate and assumes continuity of the function and its derivatives.

b) Tomographic Reconstruction

A new ART code based on the iterative refinement method of least squares solution for tomographic interferometry was developed. Three dimensional field of the refractive index was reconstructed from the optical path data recorded on the interferograms.

The integral optical length for negligible ray curvature is expressed by the Radon transformation[3]:

$$\ell(P,\theta) = \int_{-\infty}^{+\infty}\int n(x,y)\,\delta[P-x\cos(\theta)-y\sin(\theta)]\,dxdy \qquad (1)$$

where δ is the Dirac delta-function, and the parameters P and θ define the position and the orientation of the ray. The interferograms provide data on the optical pathlength, $\ell(P,\theta,z_o)$, along the ray S. The reconstruction problem is to obtain the map of $n(x,y,z_o)$ from a number of angular projections. A common procedure for obtaining the reconstructed map is matrix inversion. A square grid is superimposed over the density field and the refractive index within each element (pixel) is assumed to be constant. The Radon transformation reduces to a set of discrete equations:

$$\sum_{i=1}^{m}\sum_{j=1}^{m} w_{ij}(P,\theta)\, n_{ij} = \ell(P,\theta) \qquad (2)$$

The weight factors, w_{ij}, are determined from geometric relations. Equation (2) is evaluated for N independent rays, resulting in N linear equations. N should be larger or at least equal to the number of pixels, P. The overdeterminate system of linear algebraic equations can be generated and, in principle, solved for the unknown coefficients, $n_{ij}(z_o)$.

Tomographic reconstruction of the phase object was achieved with a modified version of a well documented Algebraic Reconstruction Technique (ART). The linear equations (equation 2) were iteratively solved. Method of conjugate gradient[4] was used to maximize the rate of convergance. A more detailed account of the technique is given in Reference 5.

c) Data Reduction

A simplifying and common assumption made throughout this program has been that the effects of refractive index gradient on the beam propagation is negligible. This allowed the use of two dimensional reconstruction codes for solving for the phase map along horizontal planes. The reconstructed data consisted of the density field at any one elevation above the airfoil chord line. For perfect gas, and assuming constant static pressures for each side of the shockwave, the density data may be reduced to a velocity or mach number map.

Due to the courseness of the calculation grids (20 x 20, or 100 x 100), the position and the strength of the shock may not directly be deduced from the tomographic reconstruction results. A method was developed to extract shock position and shock strength directly from the discontinuities observed in the interferograms.

The reconstructed density field around the leading edge of the rotating blade at different heights above the rotor blade, however, showed the existence of a shock wave extending beyond the blade[6]. Determination of the location and the strength of the shock wave using the existing codes were not possible. Radon transformation in theory can only be applied to a continuous field[3]. Using an adaptive selection technique on the original interferogram data, it was possible to reconstruct the discontinuities in the phase map.

It was noted that a number of the interferograms showed discontinuous fringe patterns, representing the passage of rays through the shock wave. The regions of the interferogram where the fringe number distribution underwent a rapid change constituted the input data for the reconstruction of the shock waves.

Figure 4 shows the fringe number distribution across a shock wave. The data of Figure 2 were obtained by generating a high resolution image (150 pixels per inch) of the fringe discontinuity region. In contract, the reconstruction of the entire field of interest were achieved with a resolution of 10 pixels per inch.

Reconstruction of the shape of the shock wave and the shock strength was based on the assumption of isotropy for the two regions before and after the shock wave (denoted as the "+" and "-" regions). The relation between the flow Mach number, M, and the index of refraction, $N = n - n_\infty$ can be written as

$$M_+/M_\infty = (1 + C_1 N_+/M_\infty^2)/[1 - (\gamma-1)\, C_1 N_+]^{1/2} \qquad (3)$$

where C_1 is a constant. The normal shock assumptions and Gladstone-Dale formula relating the refractive index with the gas density can be used to relate the upstream Mach number to the refractive indices across the shock wave.

$$\frac{1 - C_1 N_-}{1 - C_1 N_+} = \frac{6M_+^2}{M_+^2 + 5} \qquad (4)$$

Discontinuous fringe patterns may only be achieved for rays parallel to the shock wave for any finite length. The optical path difference between rays 1 and 2 is determined by

$$C_2 L_S (N_+ - N_-) = \Delta F \qquad (5)$$

where L_S is the length of the shock wave element parallel to the rays, ΔF is the fringe number difference at fringe discontinuity regions (see Figure 3), and C_2 is a constant.

An iterative algorithm was developed. Four unknowns, M_+, N_+, N_-, and L_S for each "shock wave zone" was calculated to satisfy the equations (3) to (5) and a fourth condition on the continuity of refractive indices around the shock wave in both regions.

2.0 SUMMARY OF THE MOST IMPORTANT RESULTS

a) Numerical Experimentation:

To evaluate the developed tomographic reconstruction code, a numerically generated density ratio field shown in Figure 5.0 was used as an input for the numerical test. It represents the calculated density distribution over the tip region of the rotor blade in a plane above the blade[7]. The data of integral optical length difference as a function of ray parameter θ and P was generated from Equation (2). The errors associated with the optical length measurement, encountered in the real tomography, were artificially added to the data file. Fringe round-off errors of ± 0.5, ± 0.05 and ± 0.005 were used here. Parametric study of the reconstruction code was achieved for different ranges of view angle and equation numbers.

The numerical test matrix is given in Table 1. Figure 6 shows the development of the reconstructed field $x_{ij,rec}$ with iteration number for Case 1. ϵ_T is defined as the average of the square of the inversion errors.

Convergence rate of the algorithm and the corresponding reconstruction errors as functions of input data errors, the projection ray numbers and the view angles were investigated

and the results are given in Figure 7. The following conclusions may be drawn from the numerical experimentation:

- The convergence rate is increased as the projection ray number, N, is increased (Figure 7a). The corresponding inversion error for sufficient number of iterations is, in general, independent of N. (Figure 7d).

- The norm of the residual vector, R, in all cases, unconditionally converges to a limit which is a strong function of the input data error (Figure 7b). The resulting error for the first few iterations is independent of the input data error (Figure 7e). However, for more accurate input data, additional iterations result in more accurate solutions. This underlines the importance of the accuracy of the data set. It also proposes a guideline for determining the optimum number of iterations based on the rate of change of the residual.

- Finally, limited viewing angles ($> 30°$) do not have a significant effect on the convergence rate or the accuracy of the reconstructed data (Figures 7e and 7f). Acceptable results were obtained for total view angles of 30°. Care must be taken to ensure that sufficient information is recorded on the interferograms, when the view angle limitations are imposed. In the present case, the projection

angles were taken to be symmetric about the axis of the blade (90° to the chord line).

b) Reconstruction of the density and velocity field.

The reconstructed density field around the leading edge of the rotating blade for heights z = 1.3, 2.5, 3.8 and 5.1 cm for a 7.5 cm chord and blade aspect ratio of 13.7 is shown in Figure 8. In each case a 20 x 20 pixel with dimensions of 10 mm by 20 mm was used. The programs were run on an IBM PC. The run time for each iteration was approximately 3 minutes, and the results are shown after 3 to 6 iterations.

The results show the existence of the shock wave extending beyond the blade. The magnitude of the maximum density ratio represents the strength of the shock wave for increasing height from the blade surface. More detailed evaluation of the flow field requires more refined mesh dimensions. The reconstructed data at z = 1.3 and 7.8 cm exhibit less noise than the middle stations. This may be attributed to the error in the input data.

The distribution of the density ratio at three longitudinal positions x/B = 0.94, 0.98, and 1.02 are shown in Figure 9. The data in all cases exhibit less than adequate sharpness in the position of the shock wave. This is also attributed to

the courseness of the reconstruction grid. Due to limited memory map, further refinement of the grid on the same microprocessor was not possible.

Figure 10 shows similar results in a form of constant density lines for z = 0.5". To transform the density field into the velocity field, accurate location of the shock wave was needed which was determined from the fringe discontinuity locations. Figure 11 shows the map of constant velocity contours. The location of the shock wave is shown as the line of discontinuity in the velocity contours.

TABLE 1. THE NUMERICAL TEST MATRIX

CASE	FRINGE NUMBER ROUND OFF ERROR	VIEW ANGLE (degree)	NUMBER OF VIEWS	NUMBER OF POINTS PER VIEW
1	0.005	0 .. 180	61	20
2	0.005	0 .. 90	61	20
3	0.005	0 .. 180	31	20
4	0.050	0 .. 180	61	20
5	0.050	0 .. 180	31	20
6	0.500	0 .. 180	61	20
7	0.500	0 .. 180	31	20
8	0.005	-75 .. 75	31	20
9	0.005	-60 .. 60	31	20
10	0.005	-45 .. 45	31	20
11	0.005	-30 .. 30	31	20
12	0.005	-15 .. 15	31	20
13	0.050	-75 .. 75	31	20
14	0.050	-60 .. 60	31	20
15	0.050	-45 .. 45	31	20
16	0.050	-30 .. 30	31	20
17	0.050	-15 .. 15	31	20

3.0 LIST OF PUBLICATIONS

Tomographic Reconstruction of Three-Dimensional Flow Over Air Foils, by D. Modarress, H. Tan, and J. D. Trolinger, AIAA 85-0479, January 1985.

Algebraic Reconstruction Technique Code for Tomographic Interferometry, by H. Tan, and D. Modarress, Optical Engineering, Vol. 24, No. 3, May-June 1985.

An Automated Holographic Interferometry Data Reduction System, by H. Tan, J. D. Trolinger, and D. Modarress, Presented at the SPIE Meeting, San Diego, 1986.

Application of Tomography in 3-D Transonic Flows, by D. Modarress, and H. Tan, to be presented at the AIAA 19th Fluid Dynamics, Plasma Dynamics, Laser Conference, June 1987.

4.0 LIST OF PARTICIPATING SCIENTIFIC PERSONNEL

Dr. Jim D. Trolinger
R&D Director and Chief Scientist
Spectron Development Laboratories

Dr. Dariush Modarress
Fluid Mechanics Group Leader
Spectron Development Laboratories

Dr. Hung Tan
Senior Scientist
Spectron Development Laboratories

5.0 REFERENCES

1. Rosenfeld, A., and A. C. Kak, "Digital Picture Processing," Academic Press, Inc., London (1982).

2. Harder, R. L., and R. N. Desmarais, "Interpolation Using Surface Splines," J. Aircraft, 9(2), 189, 1972.

3. Deans, S. R., The Radon Transform and some of its Applications, Cap. 1, Wiley, New York (1979).

4. Reid, J. K., "Large Sparse Sets of Linear Equations", J. K. Reid, ed., Academic Press, New York (1971).

5. Tan, H., and Modarress, D., "Algebraic Reconstruction Technique for Tomographic Interferometry," Optical Engineering, Vol. 24, No. 3, May - June 1985.

6. Modarress, D., Tan, H., Trolinger, J. D., Yu, Y., "Tomographic Reconstruction of Three-Dimensional Flow Over Airfoils", AIAA-85-0479 (1985).

7. Caradonna, F., "The Transonic Flow about a Helicopter Rotor," Ph.D. Dissertation, Stanford University, 1978.

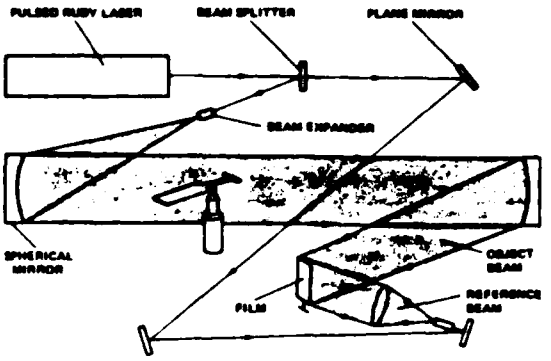

Figure 1. Basic Holographic Interferometry System.

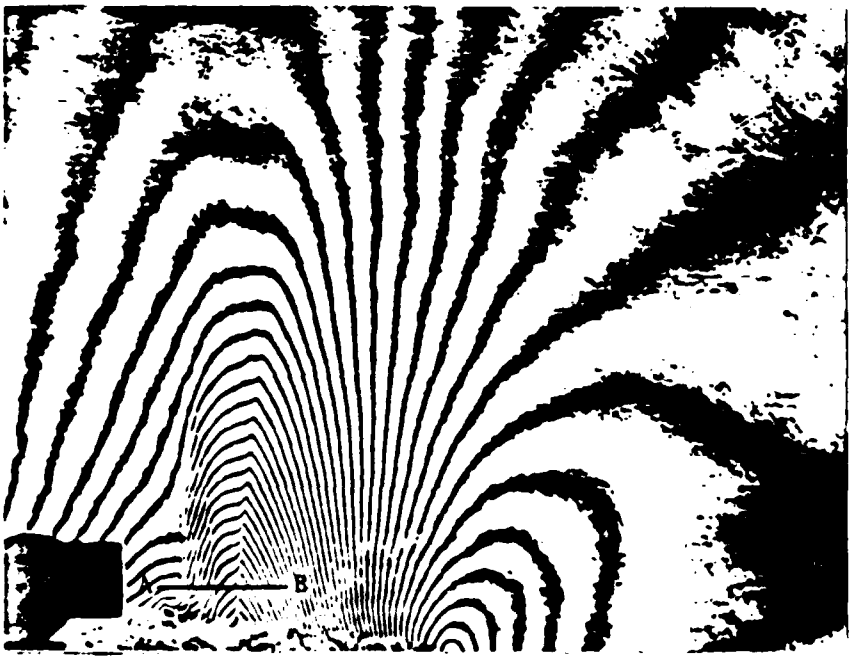

Figure 2. Holographic Interferometer, θ = 176.5°

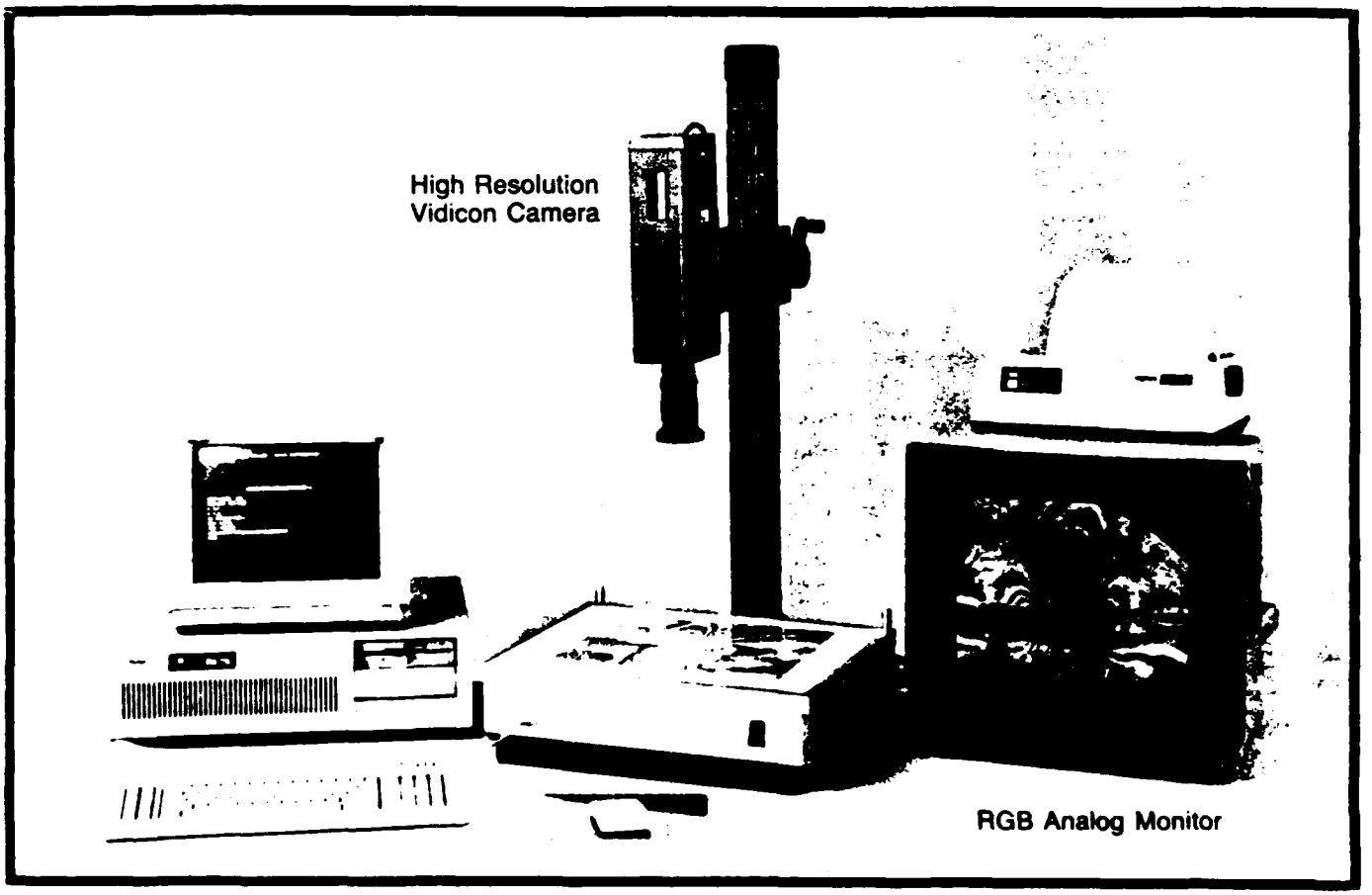

Figure 3. Fringe Digitization Hardware

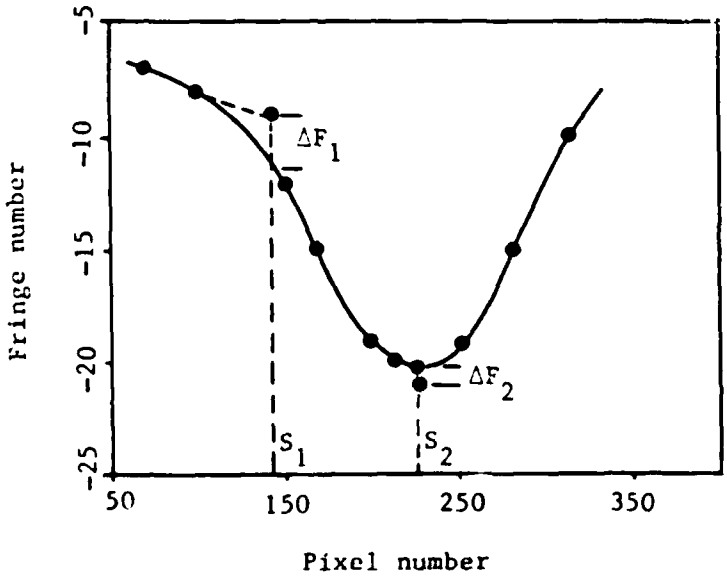

Figure 4. Fringe number distribution along line AB (of Figure 2)

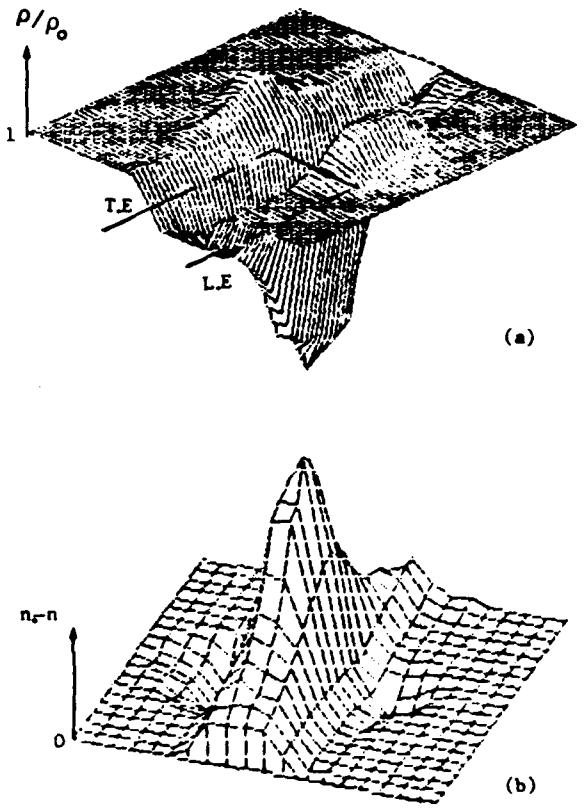

Figure 5. Numercially generated density and refractive index distribution (Ref. 7).

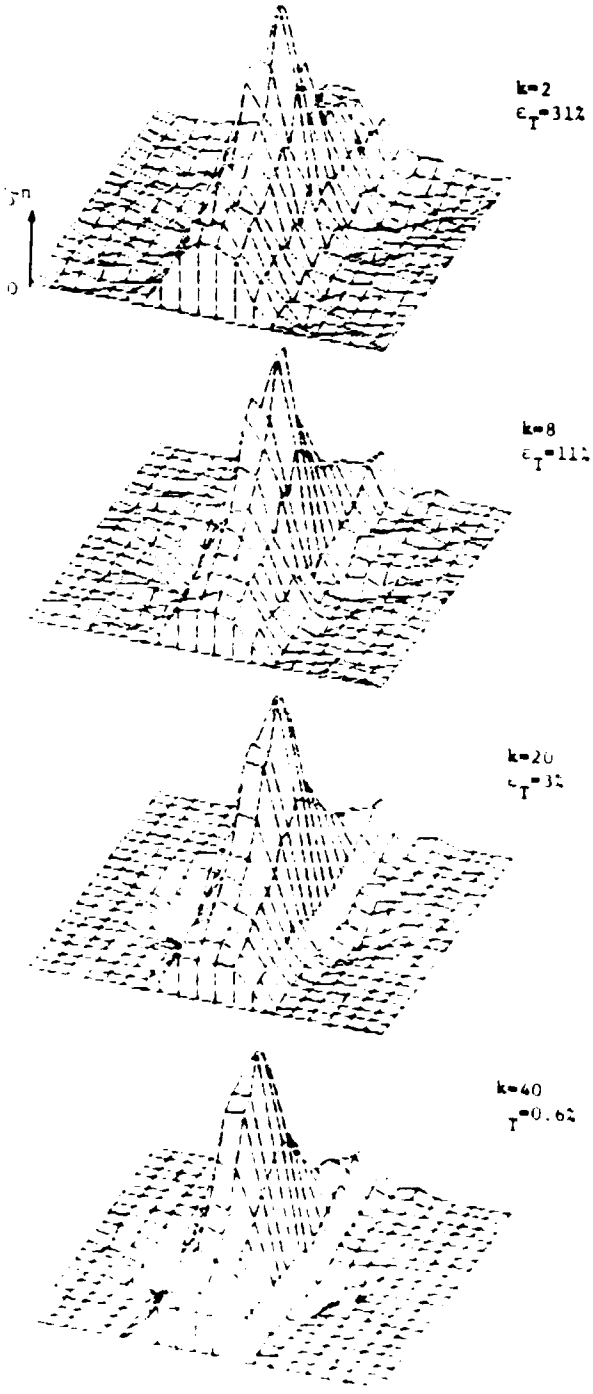

Figure 8. Reconstructed field of refractive index [illegible]

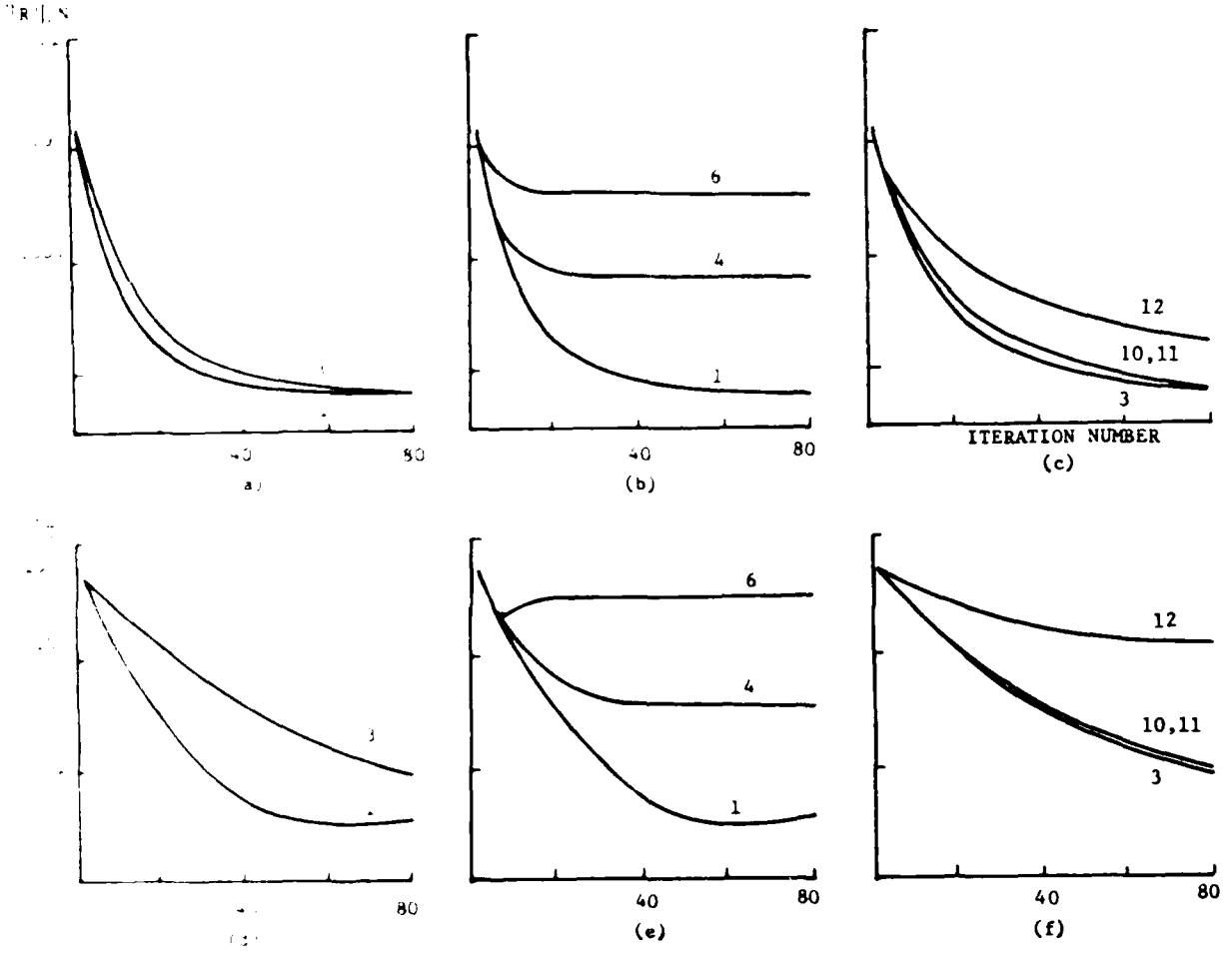

Fig. 7. Residual and conversion errors vs. iteration number for different projection ray numbers (a & d); data file errors (b & c); and total view angles (e & f). Inside numbers correspond to case numbers of Table 1.

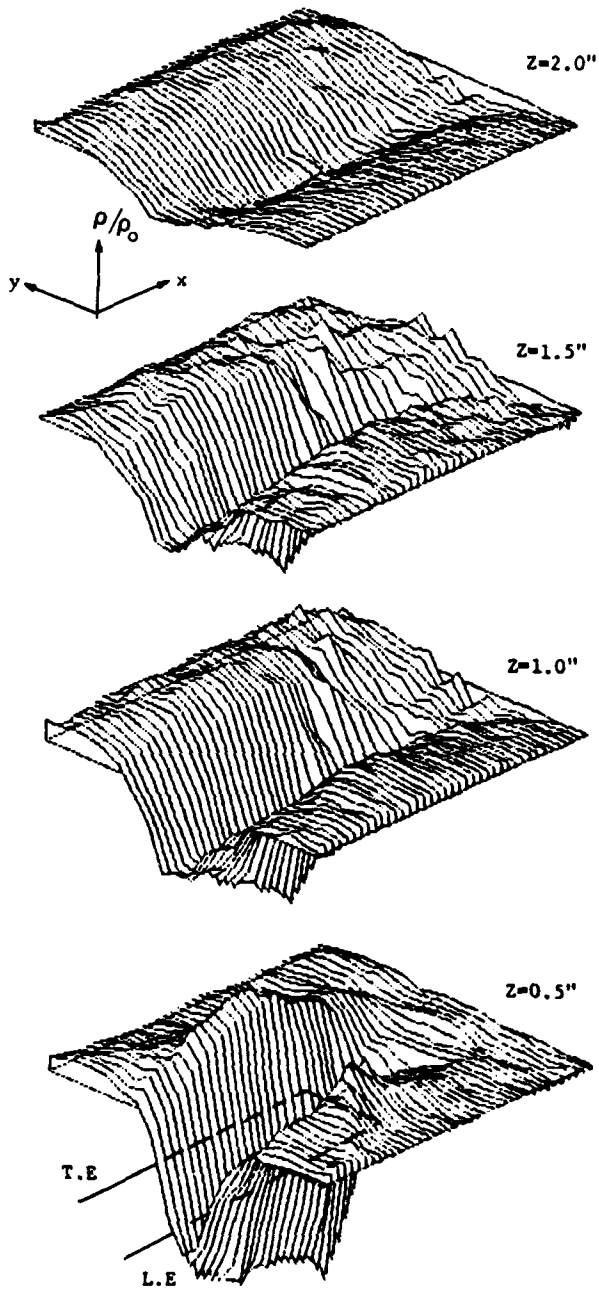

Figure 8. Reconstructed density field for different heights above blade chord line.

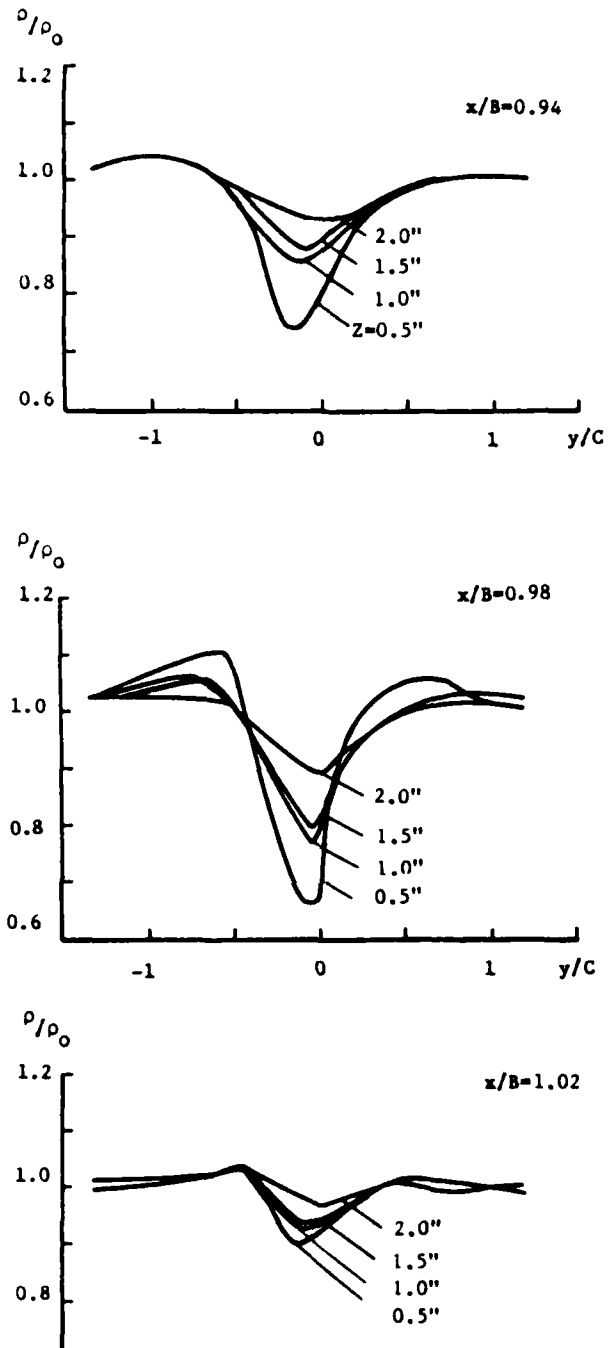

Figure 9. Density ratio profile
(B=Blade length, C=Chord length)

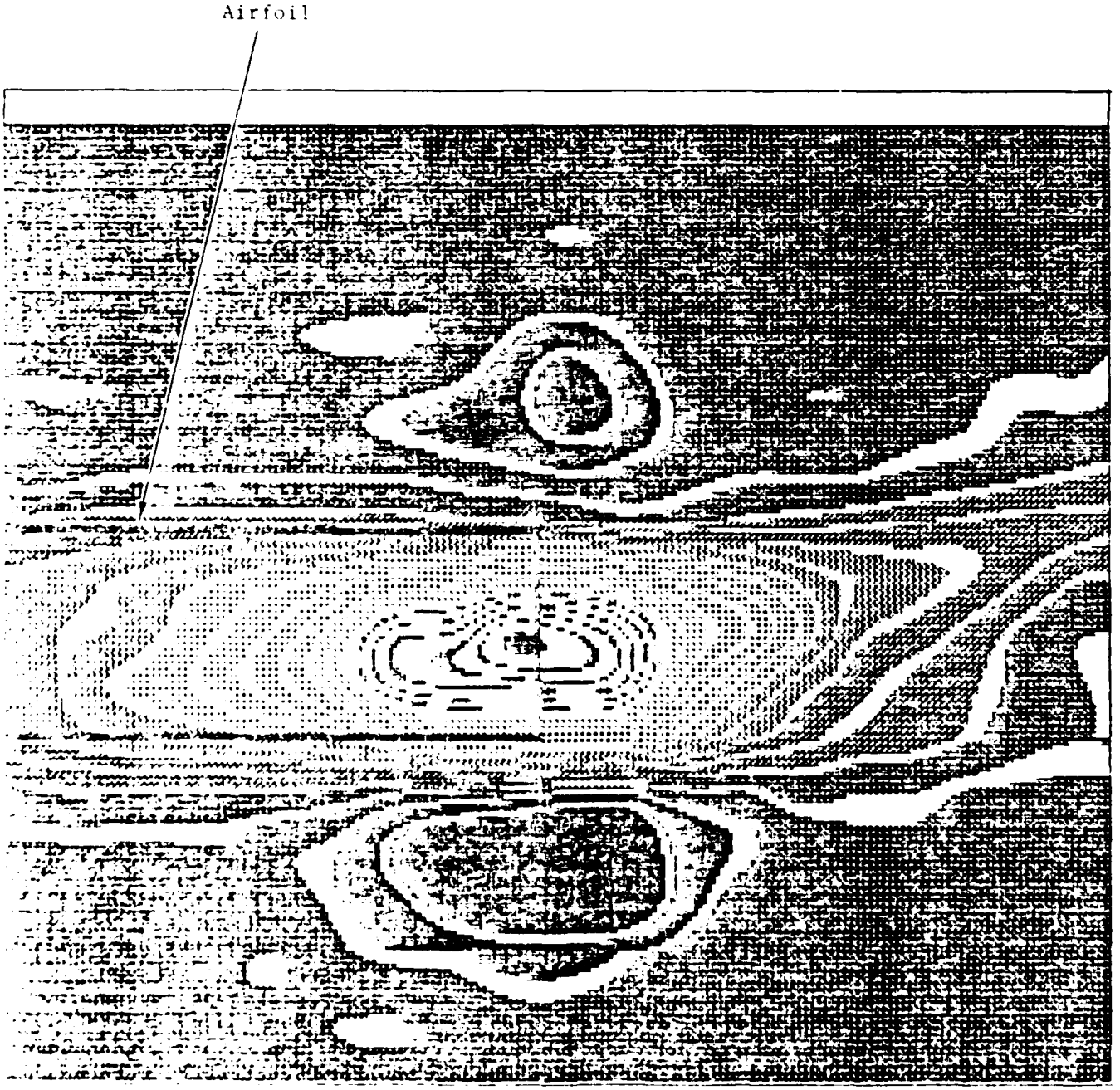

Figure 10. Presentation of air density distribution at Z = 0.5" above a rotating NACA 0012 airfoil.

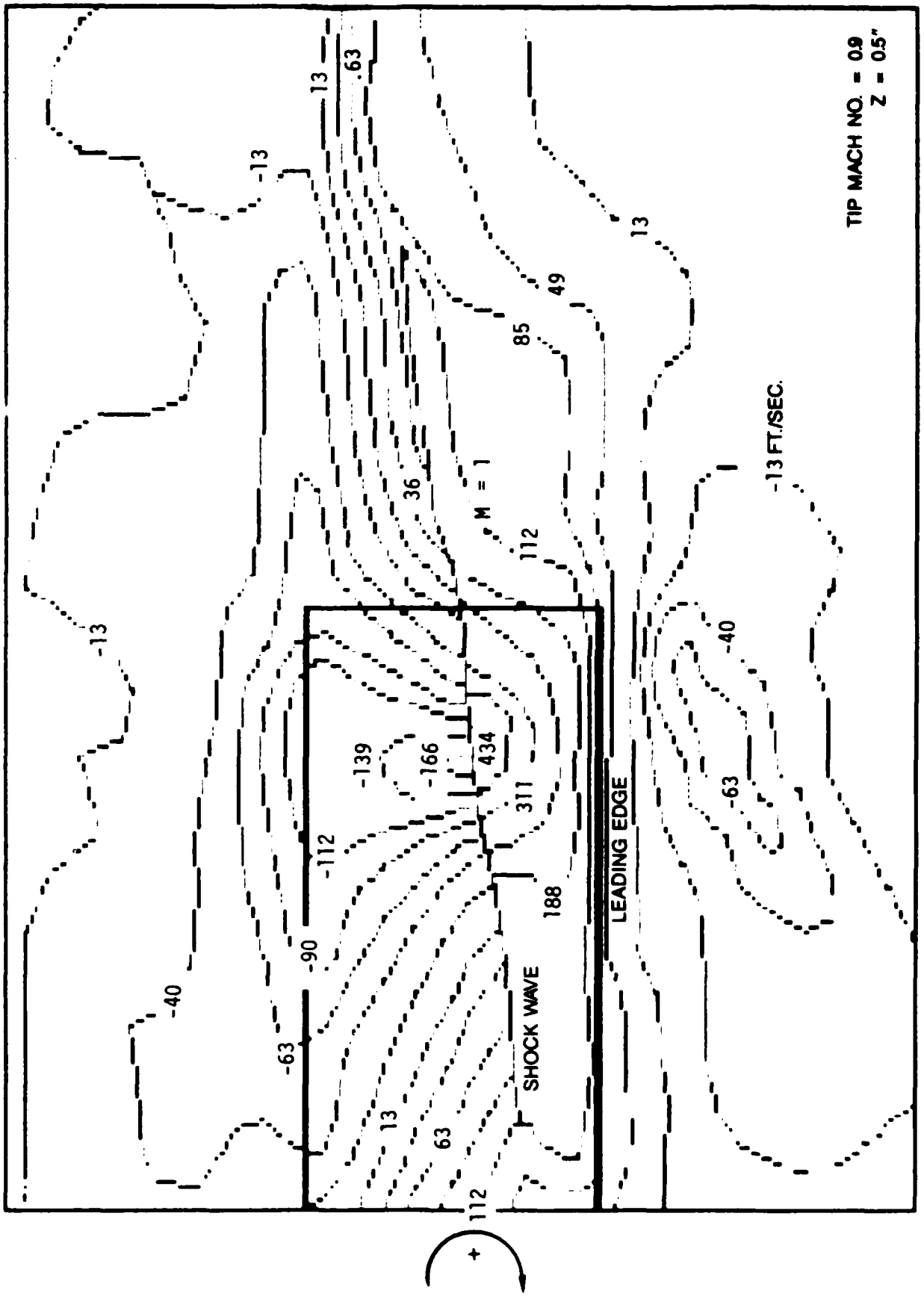

Figure 11. Reconstructed Velocity Contours

END

5-87

DTIC